ARTICLE

Magnetic Properties of $Zn_{1-x}Mn_xO$ and $Zn_{1-2x}Mn_xLi_xO$ Nano Materials

You-ming Zou*, Wei Tong, Zhe Qu

High Magnetic Field Laboratory, Chinese Academy of Sciences, Hefei 230031, China

(Dated: Received on January 1, 2011; Accepted on February 14, 2011)

$Zn_{1-x}Mn_xO$ nanorods and $Zn_{1-2x}Mn_xLi_xO$ nano-particles were synthesized by solvothermal method at 160 °C. X-ray diffraction and Raman results showed that Mn ions were well incorporated into the ZnO matrix. No magnetic hysteresis were found in the magnetization curves. The hyperfine structures were observed in electron spin resonance spectra, indicating no ferromagnetic interaction between substituted Mn ions. The co-doping of Li can only change the morphology not the magnetic properties.

Key words: ZnO, Diluted magnetic semiconductor, Paramagnetism

I. INTRODUCTION

The diluted magnetic semiconductors (DMS) have attracted much interest in the past few years as materials with both spin and charge transport properties. After GaMnAs was proven to be a DMS [1], transition metal doped ZnO was predicted as high T_c DMS [2]. Many researchers observed room temperature ferromagnetism in ZnO doped with a range of transition metal ions [3−5], while others found noferromagnetism [6−8]. It should be noted that most of the ferromagnetic samples are synthesized or annealed at high temperature. So we try to grow ZnO-based DMS at temperature as low as possible to avoid possible ferromagnetic second phase.

In this work, Mn-doped ZnO nanorods were synthesized by solvothermal method at 160 °C. X-ray diffraction (XRD) patterns and Raman spectra showed that Mn ions are well incorporated into ZnO matrix. No magnetic hysteresis were found by superconducting quantum interference device (SQUID). Meanwhile, the electron spin resonance (ESR) results proved that Mn ions in ZnO matrix do not interact with each other. Li-doping was a well-used method to increase the carrier density in ZnO. Thus the Mn and Li co-doped samples were prepared in the same procedure for comparison.

II. EXPERIMENTS

The preparation of $Zn_{1-x}Mn_xO$ nanorods are described as following. Total amount of 5 mmol $Zn(Ac)_2{\cdot}2H_2O$ and $Mn(Ac)_2{\cdot}4H_2O$ with given atomic ratios were added into 50 mL ethanol with vigorous magnetic stirring for 20 min at room temperature. The 25 mL of 1 mol/L NaOH solution in ethanol was prepared in advance and added slowly into the suspension. The suspension became once transparent and finally turbid again. The mixture was sealed in a 100 mL Teflon-lined stainless-steel autoclave and heated at 160 °C for 2 h. After cooling down to room temperature, the precipitate was washed with deionized water and absolute ethanol for several times until pH≈7 to remove NaOH and other impurities. Then the precipitate was dried in air at 60 °C, yielding the $Zn_{1-x}Mn_xO$ sample. The undoped and Li-doped samples were synthesized by the same procedure for comparison. Special precaution was taken to prevent samples from directly contacting any ferrous tools/vessels during synthesis and characterization.

The structures of $Zn_{1-x}Mn_xO$ nanorods and $Zn_{1-2x}Mn_xLi_xO$ nano-particles were determined by the XRD with Cu Kα radiation (λ=0.1542 nm) at room temperature. Field-emission scanning electron microscopy (FESEM) images and energy dispersive spectrometer (EDS) were obtained by a Sirion 200 microscope. Raman spectra were measured by a Model JY-HR800 Raman spectrometer, with the excitation wavelength of 532 nm. Magnetic properties were studied by SQUID magnetometer. The ESR spectra was measured by a Bruker EMX Plus 10/12 spectrometer.

III. RESULTS AND DISCUSSION

Figure 1 shows the XRD pattern of the $Zn_{1-x}Mn_xO$ (x=0.02 and 0.05) and $Zn_{1-2x}Mn_xLi_xO$ (x=0.05) samples. The actual Mn concentrations of these samples measured by the EDS are x=0.022, 0.053, and 0.051, respectively. The diffraction peaks of all three samples are indexed to a ZnO wurtzite structure (JCPDS No.36-1451) except for 33.1° and 60.7° in $Zn_{0.95}Mn_{0.05}O$ sample. These minor peaks should be ascribed to $ZnMn_2O_4$ (hetaerolite, JCPDS No.24-1133). The FWHM of the diffraction peak of $Zn_{0.9}Mn_{0.05}Li_{0.05}O$ sample is 0.65°, which is larger than those of $Zn_{0.95}Mn_{0.05}O$ sample

*Author to whom correspondence should be addressed. E-mail: ymzou@hmfl.ac.cn, FAX: +86-551-5595141

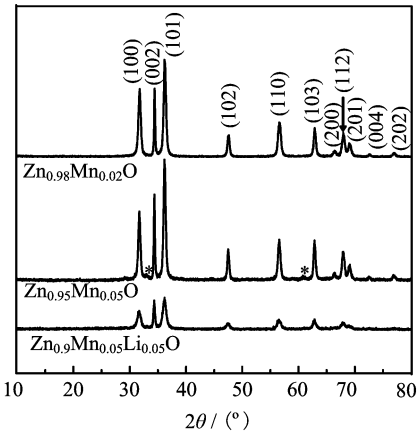

FIG. 1 XRD pattern of the $Zn_{1-x}Mn_xO$ (x=0.02 and 0.05) and $Zn_{1-x}Mn_xLi_xO$ (x=0.05) samples. The diffraction peaks (33.1° and 60.7°) denoted by "*" are indexed to $ZnMn_2O_4$.

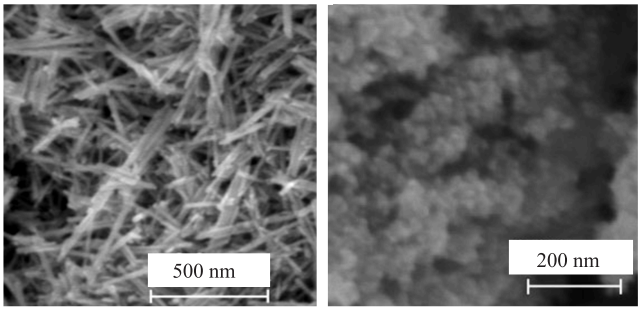

FIG. 2 FESEM images of (a) $Zn_{0.95}Mn_{0.05}O$ nanorods and (b) $Zn_{0.9}Mn_{0.05}Li_{0.05}O$ nano-particles.

(0.45°). Furthermore, the FWHM of (002) peaks are smaller than others in all samples implying that ZnO tends to grow along [002] direction and forms rod-like shape.

The $Zn_{0.95}Mn_{0.05}O$ and $Zn_{0.9}Mn_{0.05}Li_{0.05}O$ samples show different morphologies as shown in Fig.2. The $Zn_{0.95}Mn_{0.05}O$ nanorods are about 20 nm×300 nm, while the $Zn_{0.9}Mn_{0.05}Li_{0.05}O$ nano-particles are about 10 nm in diameter. A similar change of morphology is observed from pure ZnO to Li-doped ZnO. It is mentioned above that the FWHM of (002) peak is smaller than others. It is possible that the nano-particles consist of very small rod-like crystal grains.

In addition, Raman spectra (Fig.3) are measured to clarify whether Mn ions enter the right position. The Raman spectrum of the pure ZnO nanorods shows vibration modes of E_2(high)-E_2(low), A_1(TO), and E_2(high) centered at 330, 380, and 438 cm^{-1}, respectively [9, 10]. The intensity of 438 cm^{-1} peak decreased with increasing Mn concentration, which means the Mn^{2+} enter the Zn^{2+} positions and break the symmetry in ZnO host lattice. The peaks located at 476, 527, and 570 cm^{-1} are found in all Mn-doped samples, but

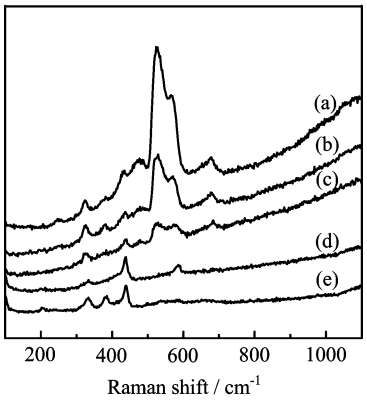

FIG. 3 Raman spectra of (a) $Zn_{0.9}Mn_{0.1}O$, (b) $Zn_{0.95}Mn_{0.05}O$, (c) $Zn_{0.9}Mn_{0.05}Li_{0.05}O$, (d) $Zn_{0.95}Li_{0.05}O$, and (e) pure ZnO.

not in pure and Li-doped ZnO. With increasing the Mn concentration, their intensity increase. The 476 cm^{-1} mode is related to an insertion of dopants in interstitial sites of the ZnO host matrix [9]. The 527 cm^{-1} peak should be ascribed to the Mn-induced disorder [11], and the 570 cm^{-1} peak is usually ascribed to the A_1(LO) phonon mode [12]. All above suggest that Mn ions are incorporated well into ZnO.

Magnetic properties of these samples are studied by SQUID and ESR. Figure 4 (a) and (b) show the M-H curves of the $Zn_{0.98}Mn_{0.02}O$ and $Zn_{0.95}Mn_{0.05}O$ samples, respectively. It is obvious that $Zn_{1-x}Mn_xO$ is paramagnetic at both room-temperature (300 K) and low-temperature (5 K), although the paramagnetic minority of $ZnMn_2O_4$ occurs in $Zn_{0.95}Mn_{0.05}O$ sample. Actually, increasing Mn content to 15% cannot yet achieve ferromagnetism. It is reported that very low doping percence of Mn (∼2%) induces a weak ferromagnetism which gets quenched if one tries ≥4% Mn doping [13]. Our samples are prepared in a different way and possibly in different carrier concentrations. Thus the ferromagnetism-paramagnetism transitions are not reproduced in our case. The Mn and Li co-doped sample are also paramagnetic as shown in Fig.4(c). It seems that the co-doping of Li does not change the magnetic interaction but obviously decrease the magnetization. The mechanism behind is not clear yet.

The ESR can provide more information about microscopic magnetic property than the SQUID. Figure 4(d) are the ESR spectra of the $Zn_{0.95}Mn_{0.05}O$ and $Zn_{0.9}Mn_{0.05}Li_{0.05}O$ samples measured at 5 K, respectively. It is shown that each spectrum has a six-line structure on the broad background paramagnetic resonance. The hyperfine structure is regarded as the fingerprint of non-interacting Mn^{2+} in wurtzite ZnO [14]. Thus, we can suggest that there are no ferromagnetism in our samples. Moreover, the hyperfine splitting (ΔH_{pp}=79 Gauss) is in close agreement with the bulk value for dilute Mn in ZnO matrix (ΔH_{pp}=76 Gauss)

DOI:10.1088/1674-0068/24/03/340-342

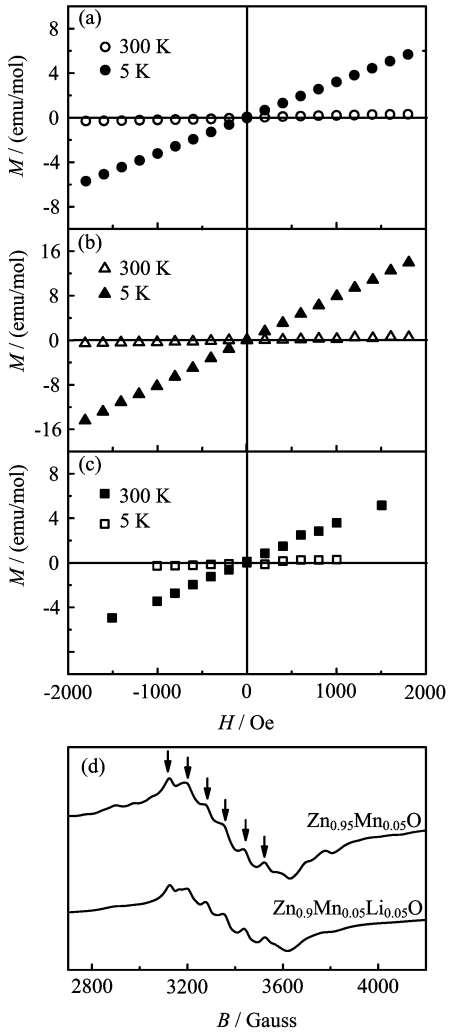

FIG. 4 Magnetization curves of (a) $Zn_{0.98}Mn_{0.02}O$ nanorods (b) $Zn_{0.95}Mn_{0.05}O$ nanorods, and (c) $Zn_{0.9}Mn_{0.05}Li_{0.05}O$ nano-particles. (d) The ESR spectra measured at 5 K, the hyperfine lines are denoted by arrows.

and precludes the occurrence of surface state Mn^{2+} atoms ($\Delta H_{pp}\approx$90 Gauss) [15]. These results, along with the Raman results, prove the successful doping of Mn^{2+} into the host lattice of ZnO. But the substitution of Mn is not the sufficient condition to introduce ferromagnetism. Co-doping of Li can't establish the interaction between Mn ions too. Although the mechanism of carrier-mediated ferromagnetism [16] is supported by many works, it is not suitable for our low-temperature-derived samples.

IV. CONCLUSION

In summary, $Zn_{1-x}Mn_xO$ nanorods were synthesized by solvothermal method. Mn^{2+} were well incorporated into the Zn^{2+} position. No ferromagnetism was found in the samples. The hyperfine structures were observed in ESR spectra, implying that the Mn^{2+} in ZnO were isolated. The co-doping of Li can change only the morphology not the magnetic properties. The origin of ferromagnetism in ZnO-based DMS is far to be understood and requires further research.

V. ACKNOWLEDGMENT

This work was supported by the National Natural Science Foundation of China (No.50702060).

[1] H. Ohno, A. Shen, F. Matsukura, A. Oiwa, A. Endo, S. Katsumoto, and Y. Iye, Appl. Phys. Lett. **69**, 363 (1996).
[2] T. Dietl, H. Ohno, F. Matsukura, J. Cibert, and D. Ferrand, Science **287**, 1019 (2000).
[3] P. Sharma, A. Gupta, K. V. Rao, F. J. Owens, R. Sharma, R. Ahuja, J. M. O. Guillen, B. Johansson, and G. A. Gehring, Nature Mater. **2**, 673 (2003).
[4] J. M. D. Coey, M. Venkatesan, and C. B. Fitzgerald, Nature Mater. **4**, 173 (2005).
[5] J. R. Neal, A. J. Behan, R. M. Ibrahim, H. J. Blythe, M. Ziese, A. M. Fox, and G. A. Gehring, Phys. Rev. Lett. **96**, 197208 (2006).
[6] J. Luo, J. K. Liang, Q. L. Liu, F. S. Liu, Y. Zhang, B. J. Sun, and G. H. Rao, J. Appl. Phys. **97**, 086106 (2005).
[7] J. Alaria, M. Bouloudenine, G. Schmerber, S. Colis, A. Dinia, P. Turek, and M. Bernard, J. Appl. Phys. **99**, 08M118 (2006).
[8] M. Bouloudenine, N. Viart, S. Colis, and A. Dinia, Catal. Today **113**, 240 (2006).
[9] T. L. Phan, S. C. Yu, R. Vincent, H. M. Bui, T. D. Thanh, V. D. Lam, and Y. P. Lee, J. Appl. Phys. **108**, 044910 (2010).
[10] T. C. Damen, S. P. S. Porto, and B. Tell, Phys. Rev. **142**, 570 (1966).
[11] S. Venkataraj, N. Ohashi, I. Sakaguchi, Y. Adachi, T. Ohgaki, H. Ryoken, and H. Haneda, J. Appl. Phys. **102**, 014905 (2007).
[12] V. E. Kaydashev, E. M. Kaidashev, M. Peres, T. Monteiro, M. R. Correia, N. A. Sobolev, L. C. Alves, N. Franco, and E. Alves, J. Appl. Phys. **106**, 4 (2009).
[13] R. K. Singhal, M. S. Dhawan, S. K. Gaur, S. N. Dolia, S. Kumar, T. Shripathi, U. P. Deshpande, Y. T. Xing, E. Saitovitch, and K. B. Garg, J. Alloys Compd. **477**, 379 (2009).
[14] A. Hausmann and H. Huppertz, J. Phys. Chem. Solids **29**, 1369 (1968).
[15] G. Clavel, M. G. Willinger, D. Zitoun, and N. Pinna, Adv. Funct. Mater. **17**, 3159 (2007).
[16] D. Mukherjee, T. Dhakal, H. Srikanth, P. Mukherjee, and S. Witanachchi, Phys. Rev. B **81**, 205202 (2010).

DOI:10.1088/1674-0068/24/03/340-342